COMPDYN 2019
7th ECCOMAS Thematic Conference on
Computational Methods in Structural Dynamics and Earthquake Engineering
M. Papadrakakis, M. Fragiadakis (eds.)
Crete, Greece, 24–26 June 2019

ASSESSMENT OF THE RESISTANCE MODEL UNCERTAINTIES IN PLANE STRESS NLFEA OF CYCLICALLY LOADED REINFORCED CONCRETE SYSTEMS

D. Gino[1], P. Castaldo[2], A. Dorato[3] and G. Mancini[4]

[2] Department of Structural, Geotechnical and Building Engineering (DISEG), Politecnico di Torino, Turin, Italy
corso Duca degli Abuzzi 24, 10129 Torino, ITALY
e-mail: diego.gino@polito.it

[2] Department of Structural, Geotechnical and Building Engineering (DISEG), Politecnico di Torino, Turin, Italy
corso Duca degli Abuzzi 24, 10129 Torino, ITALY
e-mail: paolo.castaldo@polito.it

[2] Department of Structural, Geotechnical and Building Engineering (DISEG), Politecnico di Torino, Turin, Italy
corso Duca degli Abuzzi 24, 10129 Torino, ITALY
e-mail: alessandro.dorato@polito.it

[2] Department of Structural, Geotechnical and Building Engineering (DISEG), Politecnico di Torino, Turin, Italy
corso Duca degli Abuzzi 24, 10129 Torino, ITALY
e-mail: giuseppe.mancini@polito.it

Abstract

The present work is devoted to estimate the resistance model uncertainty within plane stress non-linear finite element analyses (NLFEAs) of reinforced concrete structures subjected to cyclic loads. Specifically, various shear walls experimentally tested are considered for the investigation. The comparison between the plane stress NLFE structural model results and the experimental outcomes is carried out considering the possible modelling hypotheses available to describe the mechanical behaviour of reinforced concrete members subjected to cyclic loads. Several NLFE structural models are defined for each experimental test in order to investigate the resistance model uncertainty.

Keywords: model uncertainties, NLFEAs, reinforced concrete structures, modeling hypotheses, cyclic loads.

1 INTRODUCTION

In the last decades, non-linear finite element analyses (NLFEAs) have increasingly become the most common and practical instruments able to model the actual mechanical behaviour of structural systems, such as reinforced concrete elements, in any loading condition (i.e., service limit state (SLS) and ultimate limit state (ULS)). In this context, although several guidelines for NLFEAs have been recommended by [1]-[4] in order to assure an accurate calibration and definition of the structural FE model, the results from such complex modelling need to be properly processed in order to satisfy safety and reliability requirements for engineering purposes [5]-[6]. To this aim, Bayesian finite elements have been proposed by [7] to take into account the model uncertainties for structural analysis. Contextually, different safety formats for NLFEAs have been proposed and commented in literature by several authors [8]-[13] and international codes [14]-[15] as well as their applications have been discussed by [16]-[18]. In these safety formats, uncertainties regarding the material (i.e., aleatory uncertainties) and the definition of the structural model (i.e., epistemic uncertainties) should be properly addressed in order to derive reliability-consistent design values of the global structural resistances. With regard to the material uncertainty, the corresponding randomness is usually well known and assessed, whereas the model uncertainty (i.e., uncertainty mainly related to the definition of the resistance model) associated with NLFEAs is not typically simple to be evaluated due to the different modelling hypotheses for the definition of a non-linear FE structural model. In fact, the prediction of the actual structural response through NLFEAs is characterized by a certain level of uncertainty because any numerical model aims to describe the essential characteristics of the overall behaviour neglecting other aspects.

All the research studies evidence the need to assess the model uncertainties by means of a comparison between simulations and experimental outcomes with the consequence that an in-depth characterization of the model uncertainties for NLFEAs of reinforced concrete structures is necessary to incorporate their effects on the global structural resistance assessment within the safety formats for cyclic loads. However, the assessment of the model uncertainties for calibration of a partial safety factor should also considers the different modelling hypotheses to run NLFEAs due to the different assumptions regarding the parameters that govern the equilibrium, kinematic compatibility and constitutive equations in dynamic conditions. In fact, different choices related to the described above parameters may lead to discordant results (i.e., epistemic uncertainty [19]).

With this aim, this work compares different experimental tests known from the literature [20]-[22], concerning different walls having different behaviours and failure modes in terms of global structural resistance with the numerical outcomes achieved by means of appropriate two-dimensional non-linear FE structural models (i.e., plane stress configuration). Several non-linear FE structural models are defined for each experimental test in order to investigate the influence of the model uncertainties on 2D NLFEAs of reinforced concrete members. Precisely, the assessment of the resistance modelling uncertainties in 2D NLFEAs, that belong to the group of the epistemic uncertainties, is herein based on the definition of eighteen (18) plausible structural models using different types of software and different mechanical behaviours for the reinforced concrete elements (i.e., modelling hypotheses [19]) in dynamic conditions.

2 RESISTANCE MODEL UNCERTAINTIES FOR NLFEAS

In general, the uncertainties in structural engineering can be classified in two families: aleatory and epistemic [19]. The aleatory uncertainties concern the intrinsic randomness of the variables that governs a specific structural problem, whereas the epistemic uncertainties are mainly related to the lack of knowledge in the definition of the structural model [19],[23]-[25] and sometimes represented also by auxiliary non-physical variables/choices [19]. The safety assessment of a structural system by means of NLFEAs should account for explicitly both these sources of uncertainty.

Within the semi-probabilistic limit state method [26]-[28], the safety assessment of a structural system requires a reliable definition and characterization of the structural resistances, which increasingly often derive from NLFEAs. For this purpose, different safety formats have been proposed in the literature [8]-[15]. In particular, EN 1992 [14] defines a safety format based on the definition of the partial safety factors descending from representative values and design values of the material strengths (i.e., concrete compressive strength and reinforcement steel yielding strength). While, *fib* Model Code 2010 [15] provides three different methodologies for the assessment of the structural reliability: the probabilistic method, the global resistance method and the partial factor method. These different safety formats (with the exception for the partial factor method) allow the estimation of the design structural resistance R_d, that represents the global structural resistance of a structure with its behaviour and failure mode, as expressed by Eq.(1):

$$R_d = \frac{R_{rep}}{\gamma_R \gamma_{Rd}} \tag{1}$$

where R_{rep} denotes the value representative of the global structural resistance estimated by means of NLFEAs and in compliance with the selected safety format, γ_R is the partial safety factor accounting for the randomness of material properties (i.e., aleatory uncertainties) and γ_{Rd} represents the partial safety factor related to the modelling uncertainties (i.e., epistemic uncertainties). Therefore, the aleatory uncertainties are separated from the epistemic uncertainties within *fib* Model Code 2010 safety formats for NLFEAs [8],[15]. The procedure for the estimation of the partial factor γ_R is suggested by the corresponding safety format. Conversely, the value of the partial safety factor for the resistance model uncertainties γ_{Rd} remains an object of investigation. More recently, *fib* Model Code 2010 [15] has suggested to assume different values of γ_{Rd} depending on the level of validation of the structural model. The γ_{Rd} factor equal to 1 may be adopted for models with no epistemic uncertainties (i.e., presence of evidences of model validation in the actual design conditions [15]).

However, when NLFEAs have to be performed for dynamic simulations on structures having more complex geometry (that may differ from the simple case of the beam in the failure mode), the epistemic uncertainties related to the definition of the resistance model may be larger than expected. Therefore, an in-depth characterization of the partial safety factor γ_{Rd} needs to be addressed.

3 EVALUATION OF THE RESISTANCE MODEL UNCERTAINTIES

This section describes the methodology adopted in the present work for the assessment of the partial safety factor related to the resistance model uncertainties in the definition of 2D NLFEAs under cyclic loads. As discussed by [10],[29]-[30], the following aspects have to be considered in order to identify the resistance model uncertainties for NLFEAs:

- the database of the experimental data should contain, if possible, all the parameters necessary for the reproduction of the tests and for the definition of non-linear FE structural models; note that some information, related to the material properties, is so often missing and, in the practice, usually is derived from the available data under appropriate assumptions according to the scientific literature with an increase of the model uncertainty;

- the experimental results should be related to different typologies of structures with different failure modes;
- a probabilistic analysis of the observed model uncertainties needs to be carried out in order to define the most likely probabilistic distribution with the corresponding parameters.

In compliance with [8],[15], the resistance model uncertainty, separated from the aleatory one (Eq. (1)) and denoted as ϑ_i, can be expressed by a multiplicative law. This latter relates the i-th actual global resistance (response) estimated from an experimental test $R_i(X,Y)$ to the i-th global resistance (or response) estimated by a NLFEA $R_{NLFEA,i}(X)$ and, may be expressed as follows:

$$R_i\left(X,Y\right) \approx \vartheta_i R_{\mathrm{NLFEA},i}\left(X\right) \tag{2}$$

where X is a vector of basic variables included into the resistance model, Y is a vector of variables that may affect the resisting mechanism but are neglected in the model. Note that the unknown effects of Y variables, if present, are indirectly incorporated and covered by ϑ_i. As widely explained in the next section, different modelling hypotheses are possible to model a specific reinforced concrete structure by means of NLFEAs. A comprehensive calibration of the resistance model uncertainties for 2D NLFEAs requires to account for the different modelling hypotheses which may be selected by engineers for seismic analyses.

4 NON-LINEAR SIMULATIONS: PARAMETRIC ANALYSIS RESULTS

In this section, different experimental tests corresponding to different structural systems are considered and reproduced by means of NLFEAs. These simulations are performed considering a set of modelling hypotheses in order to estimate the resistance model uncertainties with the aim to calibrate the corresponding values of the partial safety factor within the safety formats proposed by [15]. Note that all the numerical simulations have been performed by the authors after a sensitivity/calibration analysis and this is an important requirement for the proposal of this study because leads to a reduction of the epistemic uncertainties, in other words, the designers, involved in NLFEAs for the structural verification process, should be confident with this approach. As known, the structural analysis is based on the fundamental principles of mechanics such as equilibrium, of displacement compatibility and of constitutive laws [31]. In the field of NLFEAs, these principles are attended by iterative calculation procedures which inevitably lead to a certain degree of error in the final solution. Moreover, the definition of a specific structural model [31] requires different assumptions about the parameters describing the equilibrium, kinematic compatibility, constitutive equations leading to different numerical outcomes, which may be more or less realistic. Therefore, the multiplicity of choices (i.e., epistemic uncertainties) which can be assumed during the definition of a non-linear FE model leads to have a certain degree of uncertainty in the final solution. It follows that, consistently with the framework of the safety formats for NLFEAs [14]-[15], the estimation of the partial safety factor γ_{Rd} for the resistance modelling uncertainties is necessary. Considering different experimental tests known from the literature [20]-[22], Subsection 4.1 describes the different modelling hypotheses that any engineer may assume during the computational phase. The numerical results in terms of global structural resistance from the NLFEAs are described in Subsection 4.2 and also compared to the experimental outcomes.

4.1 Different modelling hypotheses within NLFEAs

A multitude of modelling hypotheses is available to carry out 2D (plane stress) NLFEAs of reinforced concrete structures. In this work, two software [32]-[33], identified anonymously by Software A, and Software B in order to avoid advertising for the different codes, are adopted in order to reproduce the outcomes of a set of experimental tests. For each software, several choices about the hypotheses and mechanical parameters related to equilibrium, compatibility and constitutive laws can be performed. Specifically, in each software four-node quadrilateral iso-parametric plane stress finite elements, based on linear polynomial interpolation and 2x2 Gauss point's integration scheme, are used for the numerical simulations as well as the FE meshes are properly defined after a calibration procedure. The non-linear system of equations is solved by means of the standard Newton-Raphson iterative procedure based on the hypothesis of linear approximation [1]. Moreover, for each software the following main characteristics for the FE models are also assumed:

- non-linear behaviour of concrete in compression including softening with a reduction of the compression strength and shear stiffness (shear retention factor variable from a minimum value of 0.1 to a maximum value of 0.3) after cracking [34]. In detail, the mono-axial constitutive model for concrete proposed by EN 1992-1-1 [14], the constitutive model described by Model Code 1990 [15] and the constitutive model described by Thorenfeldt et al. [35] have been selected in order to fit as much as possible the experimental results with each software [32]-[33];
- smeared cracking with fixed crack direction model [36]-[38];
- tri-linear $\sigma-\varepsilon$ curve for the reinforcement steel [34];
- discrete and smeared models of the reinforcement, assuming a perfect bond between the reinforcement and the surrounding concrete [34];
- Young's modulus and tensile concrete strength, as also explained previously, are the material properties derived as a function of the experimental compressive strength, according to [27].

The summary of the main hypotheses assumed in the definition of the simulations for 2D NLFEAs, adopting Software A and B [32]-[33], is listed in Table 1.

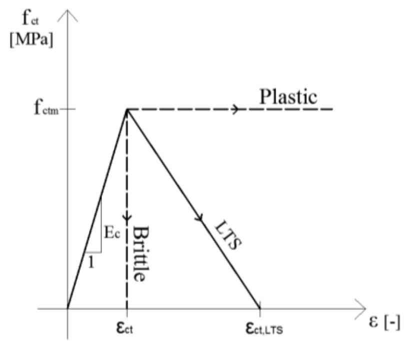

Figure 1: Different constitutive laws for concrete tensile behaviour.

In addition to the described above differences inherent to the use of two software, another important differentiation in the definition of non-linear FE models has been considered with respect to the concrete tensile mechanical behavior and the shear stiffness in cracked concrete. As known, concrete is considered as quasi-brittle material in compression and purely brittle in tension. However, the local interaction between reinforcing bars and concrete between cracks gives rise to the "tension stiffening effect" [38]. In numerical simulations, this effect may be taken into account through a modification of the constitutive tensile behavior of the concrete matrix. In general, this modification refers to the definition of a tension softening law in the post peak concrete tensile behavior. In the present paper, three different constitutive laws for concrete in tension are considered in order to cover different hypotheses accounting for the tension stiffening effect [34]: elastic-brittle, elastic-plastic and a linear tension softening as shown in Figure 1. The first two constitutive laws are conceived as upper and lower limit (non-physical) approaches. While, the constitutive law having a linear tension softening for the concrete tensile behavior represents the physical modelling hypothesis and has been calibrated by means of an iterative specific process in each software with the aim to best fit each experimental result. In this iterative process, the ultimate deformation in tensile of concrete (i.e., $\varepsilon_{ct,LTS}$ in Figure 1) is assumed as a function of the corresponding elastic one (i.e., ε_{ct} in Figure 1) varying in a range from $2\varepsilon_{ct}$ to $10\varepsilon_{ct}$ without highlighting any dependence on the software and on the compressive strength.

<table>
<tr><th></th><th>Software A</th><th>Software B</th></tr>
<tr><td>Equilibrium</td><td colspan="2">- Standard Newton-Raphson based on the hypothesis of linear approximation [1]
- Convergence criteria based on strain energy
- Load step sizes defined in compliance with the experimental procedure</td></tr>
<tr><td>Compatibility</td><td>Finite Elements
- Isoparametric plane stress 4 nodes (2x2 Gauss points integration scheme with linear interpolation)
- Discrete reinforcements
- Element size defined by means of an iterative process of numerical accuracy</td><td>Finite Elements
- Isoparametric plane stress 4 nodes (2x2 Gauss points integration scheme with linear interpolation)
- Smeared reinforcements/discrete reinforcements
- Element size defined following an iterative process of numerical accuracy</td></tr>
<tr><td>Constitutive laws</td><td colspan="2">CONCRETE
- Fixed crack model, smeared cracking, constant shear retention factor equal to:
1) 0.1
2) Variable
3) 0.3
- Mono-dimensional model extended to biaxial stress state
- Compression: Non-linear with post peak linear softening branch
- Tension (differentiating between 3 modelling hypotheses):
1) Elastic - Brittle (BRITTLE)
2) Elastic with post peak linear tension softening (LTS)
3) Elastic - perfectly plastic (PLASTIC)

REINFORCEMENTS STEEL
- Tri-linear elastic – plastic</td></tr>
</table>

Table 1: Summary of the basic hypotheses assumed in the definition of non-linear FE numerical models.

Once the tensile behavior has been established, for each of the three tensile behaviours the same investigation procedure was used to calibrate the shear retention factor (β) with a value between 0.1 and 0.3. Specifically, for each software and experimental test, three different models for the different tensile behaviour are defined and for each one 0.1 and 0.3 are imposed as limits for β, and, in addition, an iterative process is used to define the most appropriate value of β to best fit the experimental tests.

Altogether, 18 different structural models (i.e., modelling hypotheses which belong to the group of the epistemic uncertainties because a specific choice can lead to a reduction of the uncertainty [19]) can be defined combining the three different concrete tensile behaviours with the three different values of shear retention factor and the two software codes. A scheme of the modelling hypotheses adopted in this study is summarized in Figure 2. By this way, the resistance model uncertainties can be identified and computed for the different experimental tests of the 9 specimens as described in the following subsection, leading to a total number of NLFEAs equal to 162, as shown in Fig. 2.

9 specimens ⇒

Tensile behaviour	Software A			Software B		
	Shear retention factor			Shear retention factor		
	0.1	variable	0.3	0.1	variable	0.3
Brittle	Model 1	Model 2	Model 3	Model 10	Model 11	Model 12
LTS	Model 4	Model 5	Model 6	Model 13	Model 14	Model 15
Plastic	Model 7	Model 8	Model 9	Model 16	Model 17	Model 18

⇒ 162 simulations

Figure 2: Distinction between the 9 structural models (Mo.1-9 for each software) for the resistance model uncertainty investigation and summary of the benchmark NLFEAs.

4.2 NLFEAs of different experimental tests: results and comparison

In this section, the experimental results presented in the scientific literature [20]-[22] and related to 9 different r.c. walls are considered and assumed as benchmark test set. All these experimental tests, have been performed through a cyclic loading process up to failure as discussed by [20]-[22]. The specimens have been realized in laboratory and supported by statically determined configurations. The experimental results, in terms of load vs displacement, are compared to the outcomes from the different 162 2D NLFEAs carried out taking into account the resistance model uncertainties as previously discussed. It is worthy to specify that some experimental systematic errors (e.g., modifications in the geometry or in the constraints) can affect the experimental results and represent another source of uncertainties, as commented below for the comparison with some experimental results [29],[39].

In the following, the experimental and numerical tests are described in details and illustrated in Figures 3-11.

The experimental tests described by Pilakoutas and Elnashai [20], analyzed six reinforced concrete walls designed in pairs so as to have the same percentage of bending reinforcement and differing in the percentage of shear reinforcement. For this work, only 3 of the all walls have been taken into consideration denoted respectively as SW4, SW6, SW8, with the following geometrical properties: 1.20 m high, 0.6 m wide, 0.06 m thick and stiffened by a 0.2 m thick and 0.25 m high lower beam, and by a 0.2 m thick and 0.15 m high upper beam where the load is applied. All walls are subjected to the same load history. The test was carried out in displacement control from 2 mm up to failure, performing two complete cycles with a 2 mm increment. The concrete compressive strength ranges from 36.9 to 45.8 MPa in the different tests, while the flexural reinforcement remains constant in the web and the shear reinforcement and the vertical reinforcement vary in the boundary elements. The numerical results in terms of global structural resistance of the simulations are listed in Table 2 and 3. The results from NLFEAs, in Figures 3-5 (a)-(f), are plotted for the same shear hypothesis, for the different tensile behaviors and for the two software codes. The lowest results in terms of maximum load are achieved when the brittle constitutive law is adopted for concrete tensile behavior, while the plastic constitutive law always leads to an overestimation of the maximum load and of stiffness. It can also be noted that the best results are obtained for a shear retention factor of 0.1 or in any case close to this value. In general, all the simulations overestimate the maximum load and then the structural resistance, but underestimate the ductility because a lot of simulations failure before then experimental tests. Figure 3-5 (a-c) and (d-f) show the intrinsic dependence of the results on the software choice (software A and B, respectively), in which the simulations (a-c) fail the simulation before the end of the load history, while the simulations (d-f) reach the end of the analysis but they overestimate the resistance, especially in the case of the models 12, 15, 18. The failure mode occurs with the progressive yielding of the tensile reinforcements and concrete crushing in the boundary element compressed on the opposite side. This failure is in compliance with the experimental results. When the ultimate deformation for the concrete in compression is reached, all the simulations have been stopped due to the convergence loss of the numerical procedure.

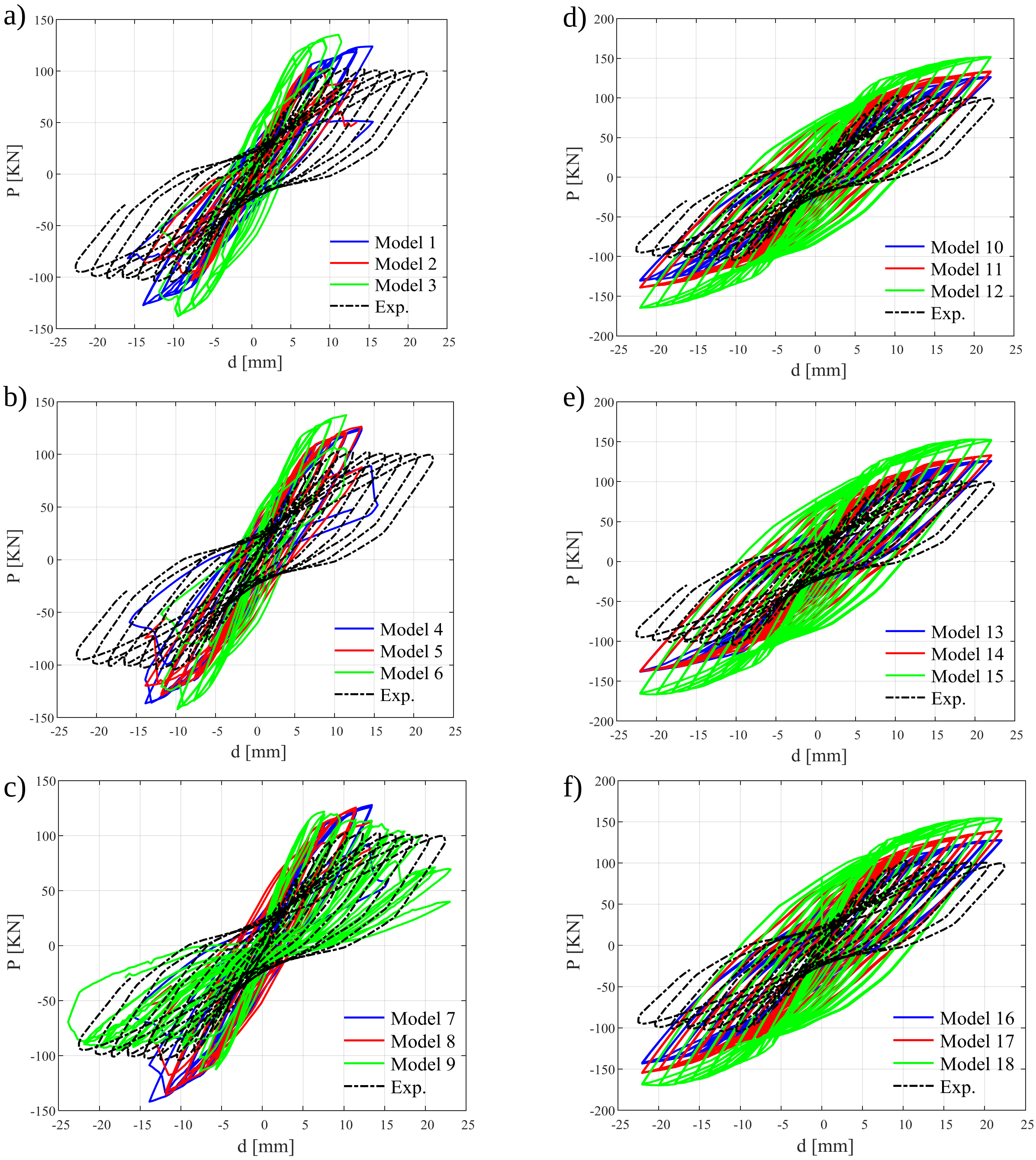

Figure 3: Load vs displacement diagrams from experimental tests SW4 of Pilakoutas [20] and NLFEA results; (a-c) Software A, (d-f) Software B.

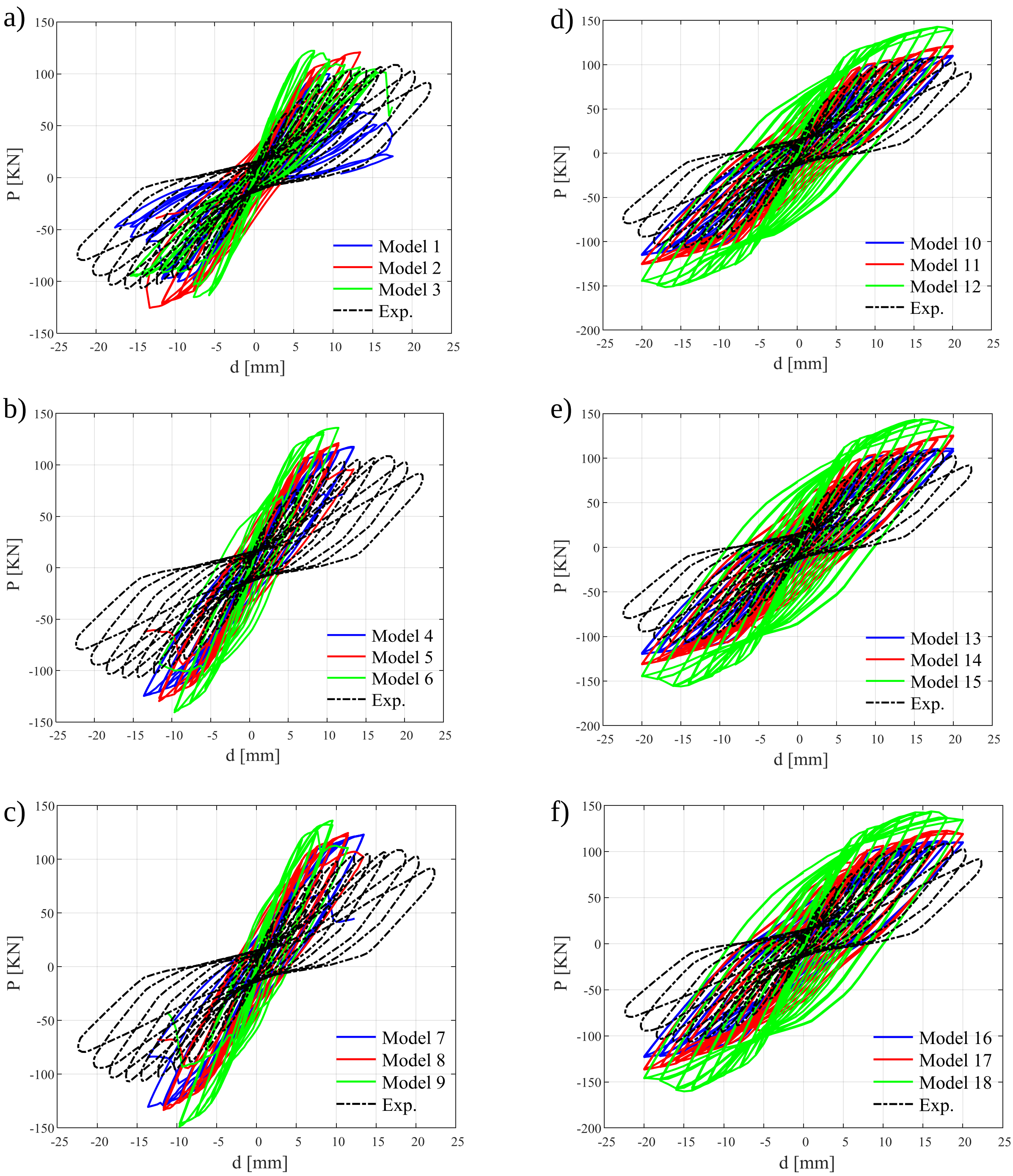

Figure 4: Load vs displacement diagrams from experimental tests SW6 of Pilakoutas [20] and NLFEA results; (a-c) Software A, (d-f) Software B.

Ref. [*]	**Exp. test**	$R_{EXP,i}$ **[kN]**	$R_{NLFEA,i}$ **[kN]**								
			Mo. 1	*Mo. 2*	*Mo. 3*	*Mo. 4*	*Mo. 5*	*Mo. 6*	*Mo. 7*	*Mo. 8*	*Mo. 9*
[20]	SW4	103.0	124.0	103.4	135.4	124.9	126.4	137.4	127.8	125.5	121.8
	SW6	108.6	100.1	120.8	122.2	117.6	121.3	134.3	123.0	124.5	136.0
	SW8	95.1	128.5	127.3	142.2	133.0	130.9	149.1	137.7	135.2	152.8

Table 2: Results in terms of resistance from the experimental tests $R_{EXP,i}$ [20] and NLFEAs $R_{NLFEA,i}$ for the different structural models, Software A.

Ref. [*]	**Exp. test**	$R_{EXP,i}$ **[kN]**	$R_{NLFEA,i}$ **[kN]**								
			Mo. 10	*Mo. 11*	*Mo. 12*	*Mo. 13*	*Mo. 14*	*Mo. 15*	*Mo. 16*	*Mo. 17*	*Mo. 18*
[20]	SW4	103.0	126.3	133.5	151.6	125.8	133.1	152.8	127.8	139.1	154.3
	SW6	108.6	110.3	121.3	142.9	110.8	125.4	142.7	111.6	122.7	143.7
	SW8	95.1	128.0	139.4	159.2	127.8	137.7	160.4	131.9	140.8	160.5

Table 3. Results in terms of resistance from the experimental tests $R_{EXP,i}$ [20] and NLFEAs $R_{NLFEA,i}$ for the different structural models, Software B.

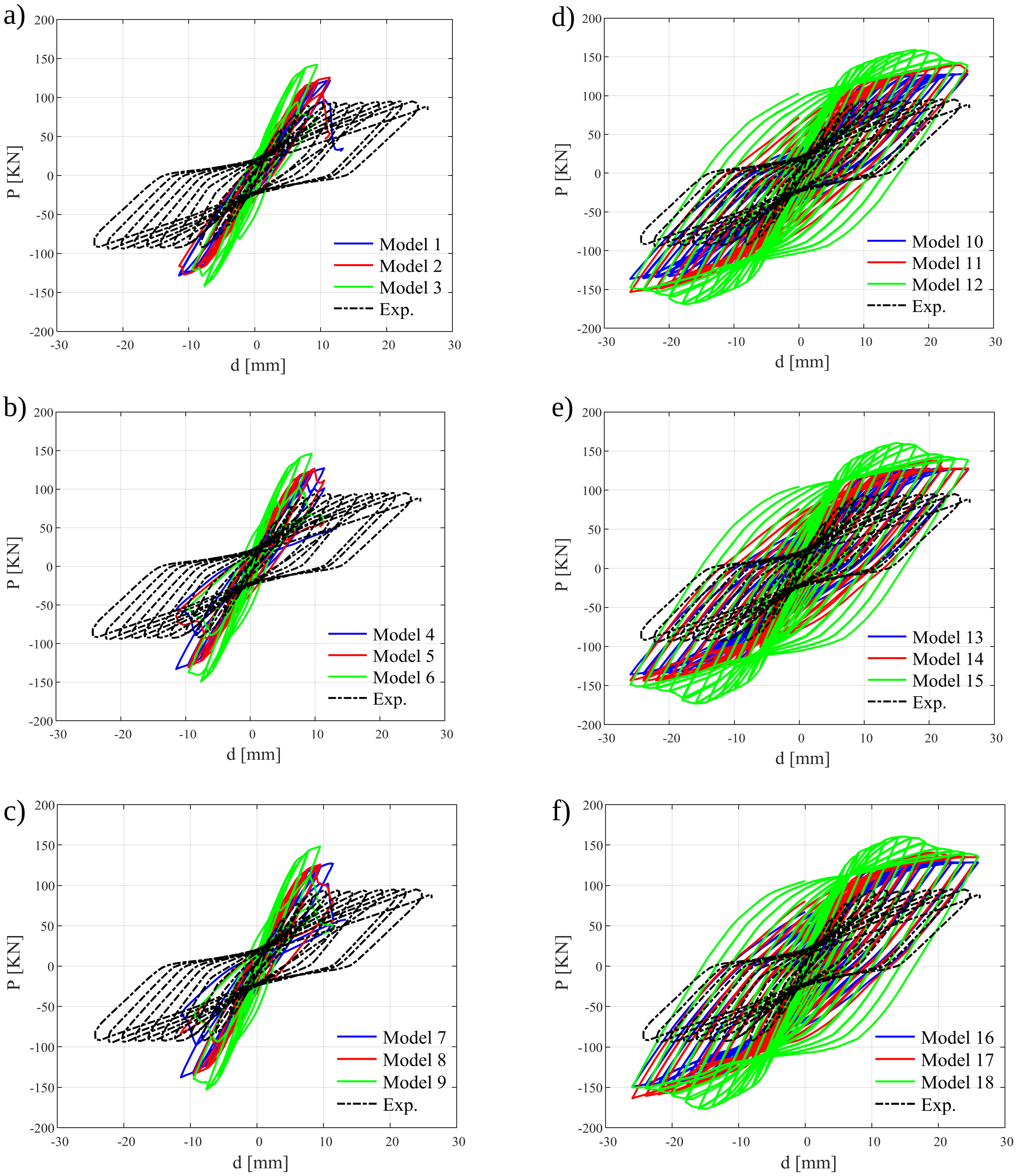

Figure 5: Load vs displacement diagrams from experimental tests SW8 of Pilakoutas [20] and NLFEA results; (a-c) Software A, (d-f) Software B.

The experimental results of Lefas and Kotsovos [21] are related to four identical walls of dimensions 1300x650x65mm, that are constrained inferiorly by a beam of section 200x300mm which simulates a rigid foundation. At the top there is a rigid beam to uniformly transmit the imposed displacement on the top of the wall. The flexural reinforcement is made up of ϕ8/100mm in the web, while the distance is reduced to 70mm in the boundary elements. Similarly, the shear reinforcement is composed of ϕ6.25/260mm over the entire width of the wall and additional stirrups in the boundary elements with ϕ4/130mm. The imposed displacement tests present a load history composed of four or five cycles with displacements of a few millimeters and then an increase of monotonic displacement up to failure. The concrete compressive strength varies in the range 35-53 MPa in the different tests. The numerical results in terms of global structural resistance of the simulations are listed in Tables 4-5. Figures 6-8 (a)-(f) show that models (3, 6, 9, 12, 15, 18) related to elastic-plastic constitutive law for the concrete tensile behavior, always lead to an overestimation of the resistance and stiffness, while models elastic-brittle and with a linear tension softening in tension have more or less the same behavior, with a stiffness similar to the real one in the cyclic phase, but, in general, an underestimation of the resistance. It can be also noted that as the shear retention factor increases, the dissipated energy also increases. The failure mode occurs with the progressive yielding of the tensile flexural reinforcements on the side where the displacement is imposed and concrete crushing at the bottom of the boundary element in the other side. Some simulations don't reach the ultimate experimental displacement but fail upon reaching the maximum load or for a slightly greater displacement than that achieved in the cyclic phase.

Ref. [*]	**Exp. test**	$R_{EXP,i}$ **[kN]**	$R_{NLFEA,i}$ **[kN]**								
			Mo. 1	*Mo. 2*	*Mo. 3*	*Mo. 4*	*Mo. 5*	*Mo. 6*	*Mo. 7*	*Mo. 8*	*Mo. 9*
[21]	SW31	115.9	111.9	120.8	160.2	121.3	133.3	168.9	127.7	139.3	174.4
	SW32	111.0	110.3	114.8	142.8	114.9	118.3	142.7	119.1	131.1	144.3
	SW33	111.5	107.2	111.5	129.8	110.4	114.0	139.4	113.8	117.6	143.8

Table 4. Results in terms of resistance from the experimental tests $R_{EXP,i}$ [21] and NLFEAs $R_{NLFEA,i}$ for the different structural models, Software A.

Ref. [*]	**Exp. test**	$R_{EXP,i}$ **[kN]**	$R_{NLFEA,i}$ **[kN]**								
			Mo. 10	*Mo. 11*	*Mo. 12*	*Mo. 13*	*Mo. 14*	*Mo. 15*	*Mo. 16*	*Mo. 17*	*Mo. 18*
[21]	SW31	115.9	87.8	117.5	139.8	98.0	127.2	147.6	98.9	131.8	151.2
	SW32	111.0	93.7	101.6	129.4	93.9	101.9	129.5	99.4	102.2	129.7
	SW33	111.5	94.6	96.0	118.7	95.2	101.1	122.8	95.7	98.8	126.9

Table 5: Results in terms of resistance from the experimental tests $R_{EXP,i}$ [21] and NLFEAs $R_{NLFEA,i}$ for the different structural models, Software B.

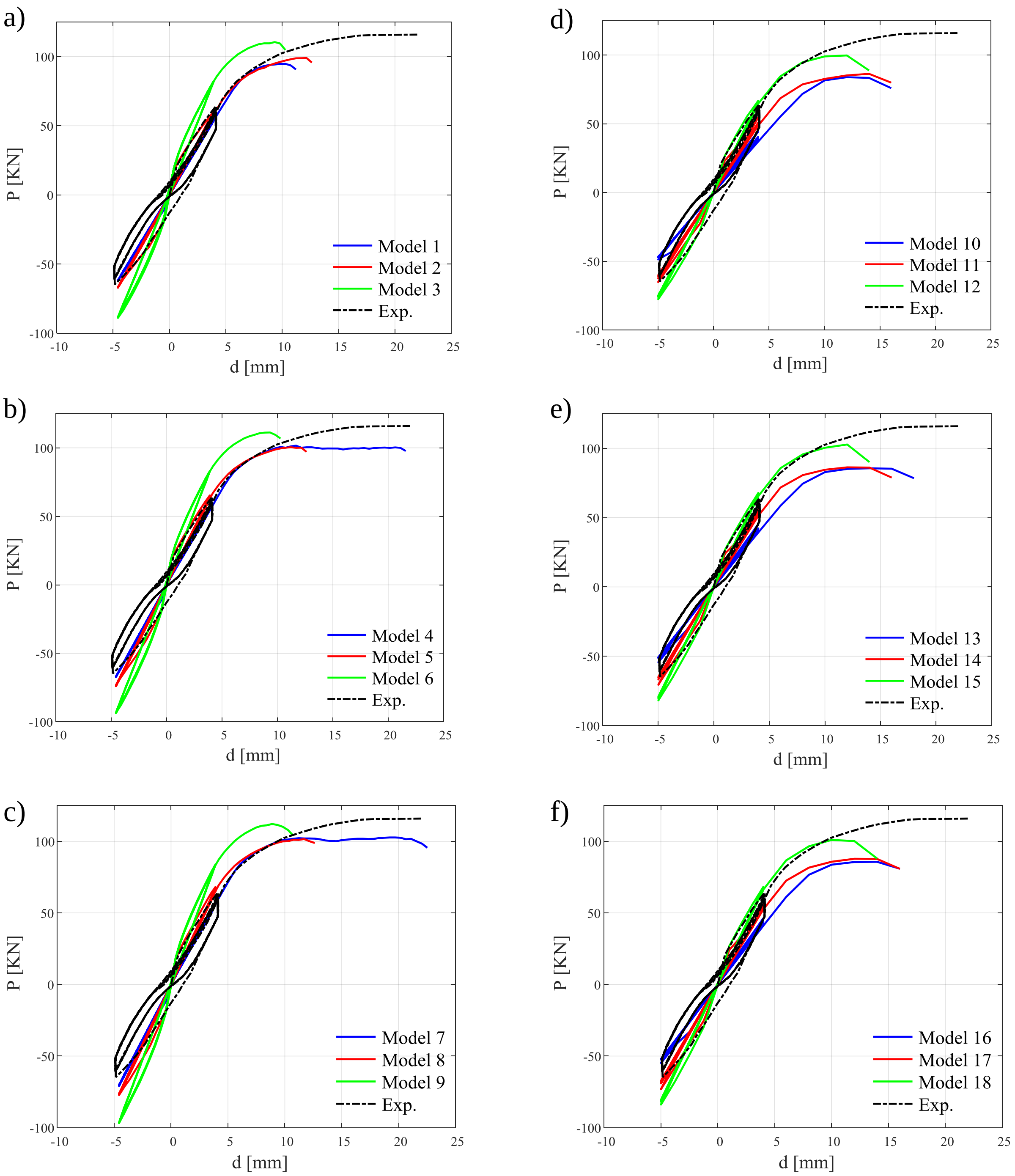

Figure 6: Load vs displacement diagrams from experimental tests SW31 of Lefas and Kotsovos [21] and NLFEA results; (a-c) Software A, (d-f) Software B.

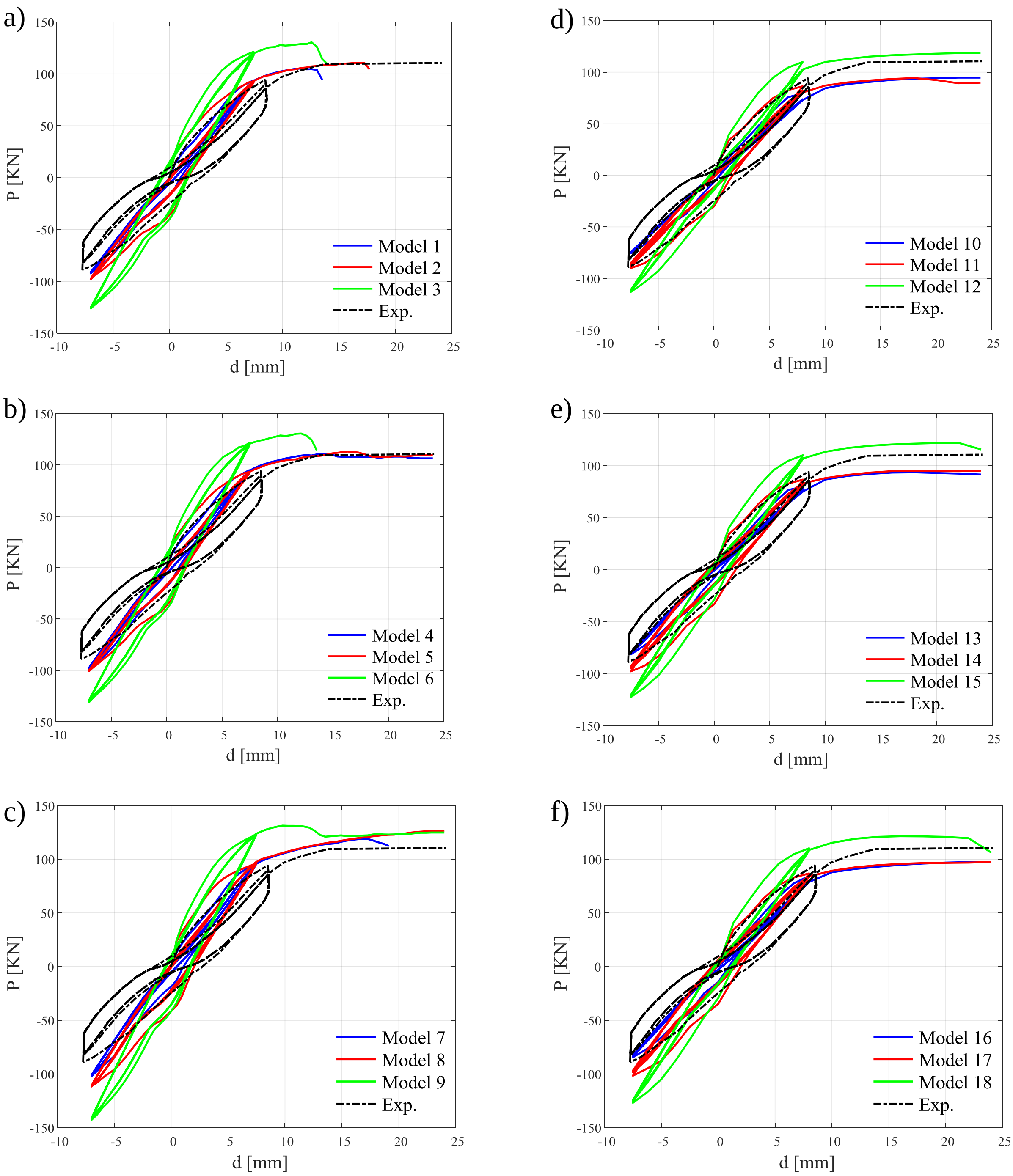

Figure 7: Load vs displacement diagrams from experimental tests SW32 of Lefas and Kotsovos [21] and NLFEA results; (a-c) Software A, (d-f) Software B.

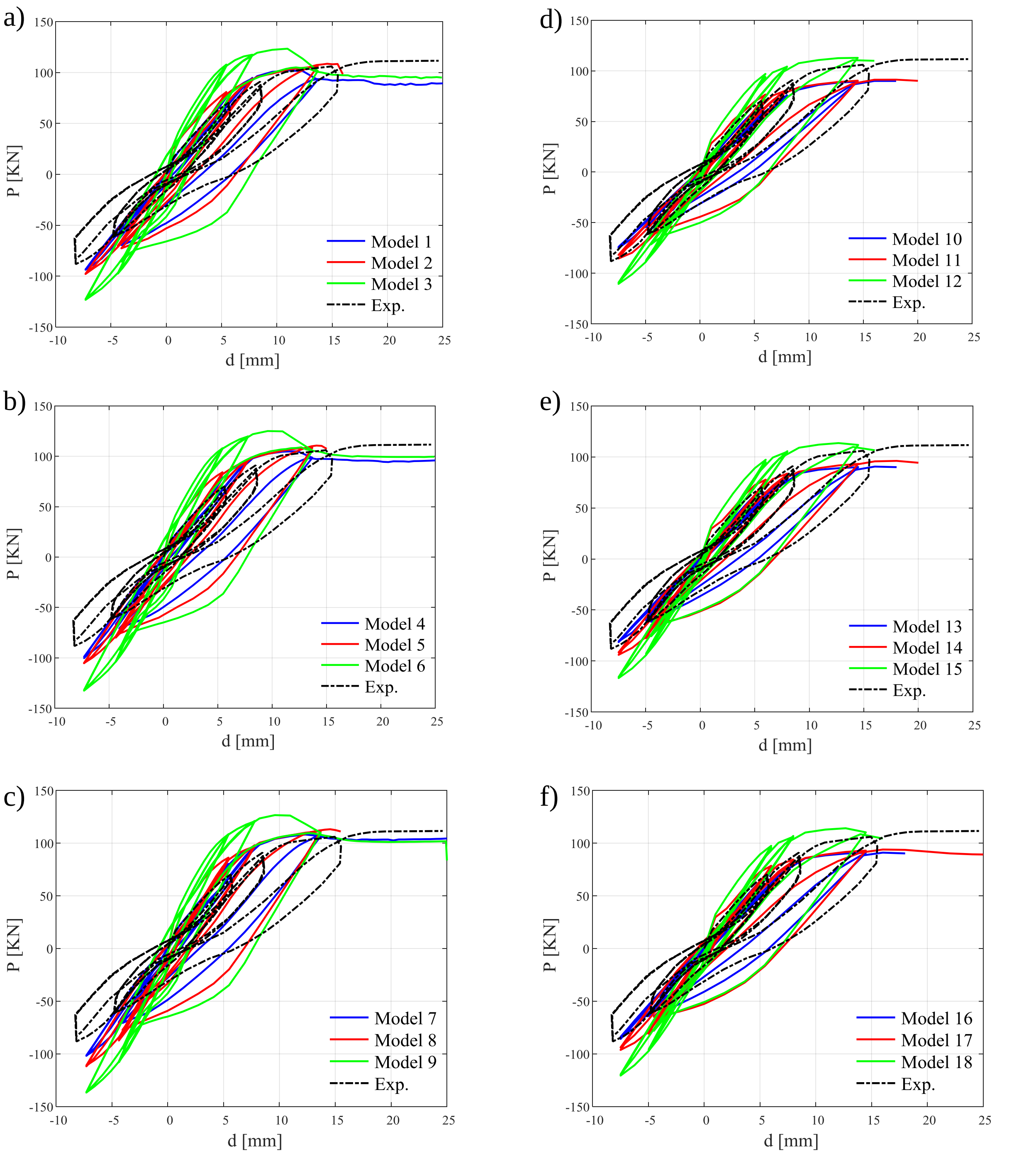

Figure 8: Load vs displacement diagrams from experimental tests SW33 of Lefas and Kotsovos [21] and NLFEA results; (a-c) Software A, (d-f) Software B.

The experimental results discussed by Zhang and Wang [22], focused on four reinforced concrete walls, denoted as SW7, SW8 and SW9 being 1.75 m high, 0.7 m wide, 0.1 m thick. The structural member is fully restrained at the base with a 0.5 m high and 0.4 m wide beam and loaded by an axial force at the top, that is considered evenly distributed at 25 cm from the top surface of the wall, while the horizontal imposed displacement is applied at 1.5 m from the base of the wall. Hence, the effective height of the wall is 1.5 m. The walls SW7 and SW8 have the same reinforcement that consist of ϕ8/150mm as flexural reinforcement in the web, while for shear ϕ8/100mm over the total width of the wall and hoops ϕ6/50mm in the boundary elements. The difference is in flexural reinforcement in the boundary elements of the wall which consists respectively of 4ϕ14 and 4ϕ12 on each side of the wall. The SW9 is more reinforced, and presents 4ϕ20 on each boundary element, and a greater amount of shear reinforcement than the previous ones with ϕ8/75mm+ ϕ6/150mm over the total width of the wall and hoops ϕ6/75mm in the boundary elements. The walls also differ in the axial load: SW7 and SW9 have an axial-load ratio of 0.24 while SW8 has a greater axial-load ratio equal to 0.35. The loading histories are quite similar and follow the same procedure: at the first time the axial load is applied in small incremental steps, after that the wall is subjected to the cyclic phase with horizontal load divided in two parts. The first consists in 10 cycles until the yielding of flexural reinforcement; in the second phase at each cycle it is proceeded with a displacement increase equal to half that recorded for yielding. The numerical results in terms of global structural resistance of the simulations are listed in Table 6-7. The NLFEA results, plotted in Figure 9-11 (a)-(f), show that models related to elastic-plastic constitutive law for the concrete tensile behavior, always lead to an overestimation of the stiffness. Models elastic-brittle in tension do not always represent the lower bound. Figure 9-11 (a-c) and (d-f) show the dependence of the results on the software choice (software A and B, respectively), in which (a-c) reflect the real behavior for small displacement and reach the experimental maximum load, while for bigger displacement there is a progressive reduction of stiffness and resistance and in many cases the simulation fails (especially for models with elastic-plastic tensile behavior). For Software B instead, in general, all the models overestimate the structural resistance, but reach the end of the loading history by following the real behavior quite well.

Ref. [*]	**Exp. test**	$R_{EXP,i}$ **[kN]**	$R_{NLFEA,i}$ **[kN]**								
			Mo. 1	*Mo. 2*	*Mo. 3*	*Mo. 4*	*Mo. 5*	*Mo. 6*	*Mo. 7*	*Mo. 8*	*Mo. 9*
[22]	SW7	201.2	189.7	195.7	206.4	203.3	202.5	209.9	212.1	206.3	224.9
	SW8	224.0	223.6	220.1	236.7	227.0	223.7	239.9	239.8	234.6	254.4
	SW9	303.5	323.6	325.0	345.0	345.7	338.1	360.4	360.4	345.3	367.4

Table 6. Results in terms of resistance from the experimental tests $R_{EXP,i}$ [22] and NLFEAs $R_{NLFEA,i}$ for the different structural models, Software A.

Ref. [*]	**Exp. test**	$R_{EXP,i}$ **[kN]**	$R_{NLFEA,i}$ **[kN]**								
			Mo. 10	*Mo. 11*	*Mo. 12*	*Mo. 13*	*Mo. 14*	*Mo. 15*	*Mo. 16*	*Mo. 17*	*Mo. 18*
[22]	SW7	201.2	226.0	223.2	241.5	240.3	236.9	255.1	252.4	249.3	264.2
	SW8	224.0	232.3	226.9	243.8	244.6	239.8	250.4	255.9	247.8	252.2
	SW9	303.5	322.7	318.1	344.4	335.1	329.2	352.3	345.1	337.4	357.4

Table 7. Results in terms of resistance from the experimental tests $R_{EXP,i}$ [22] and NLFEAs $R_{NLFEA,i}$ for the different structural models, Software B.

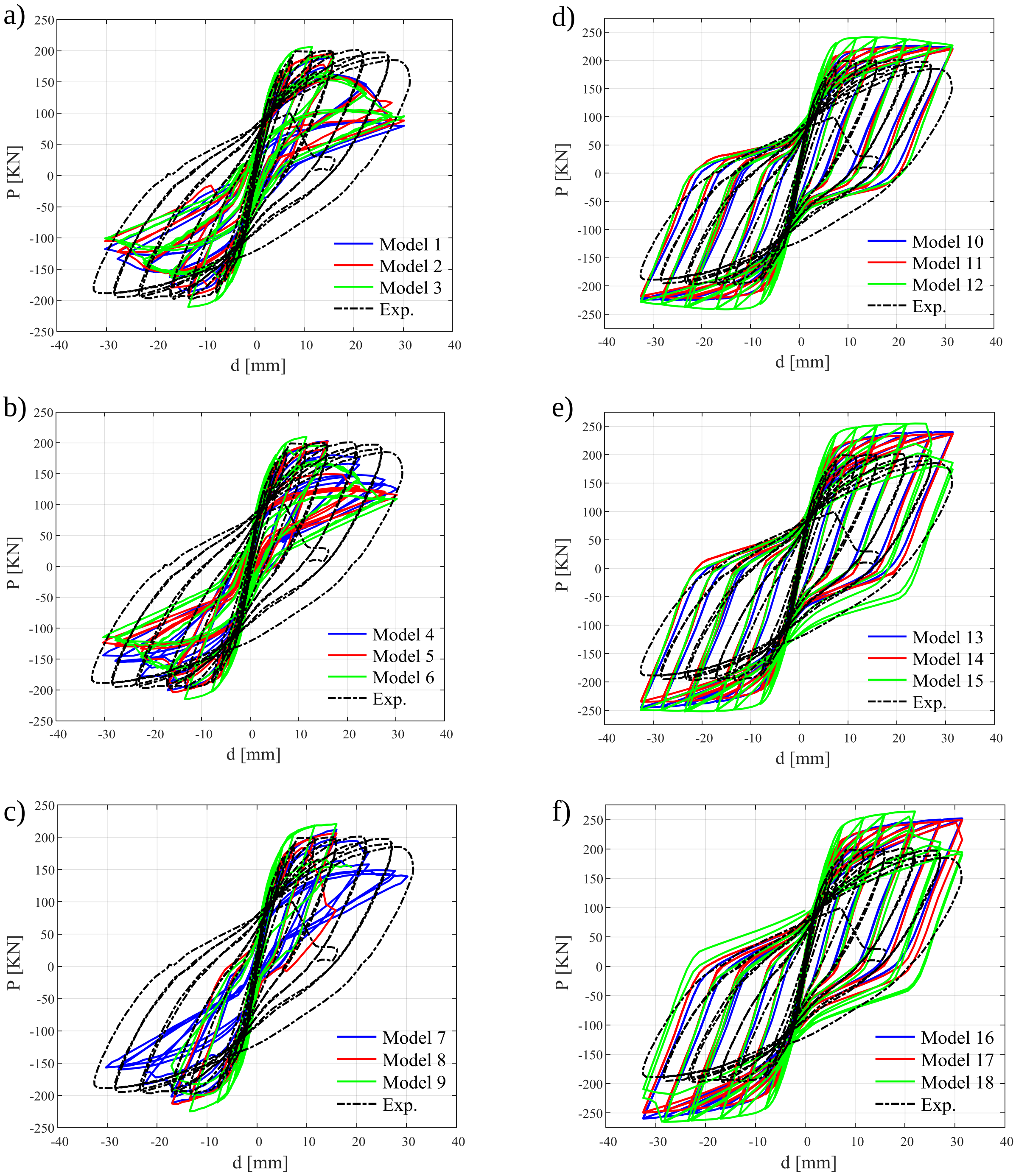

Figure 9: Load vs displacement diagrams from experimental tests SW7 of Zhang and Wang [22] and NLFEA results; (a-c) Software A, (d-f) Software B.

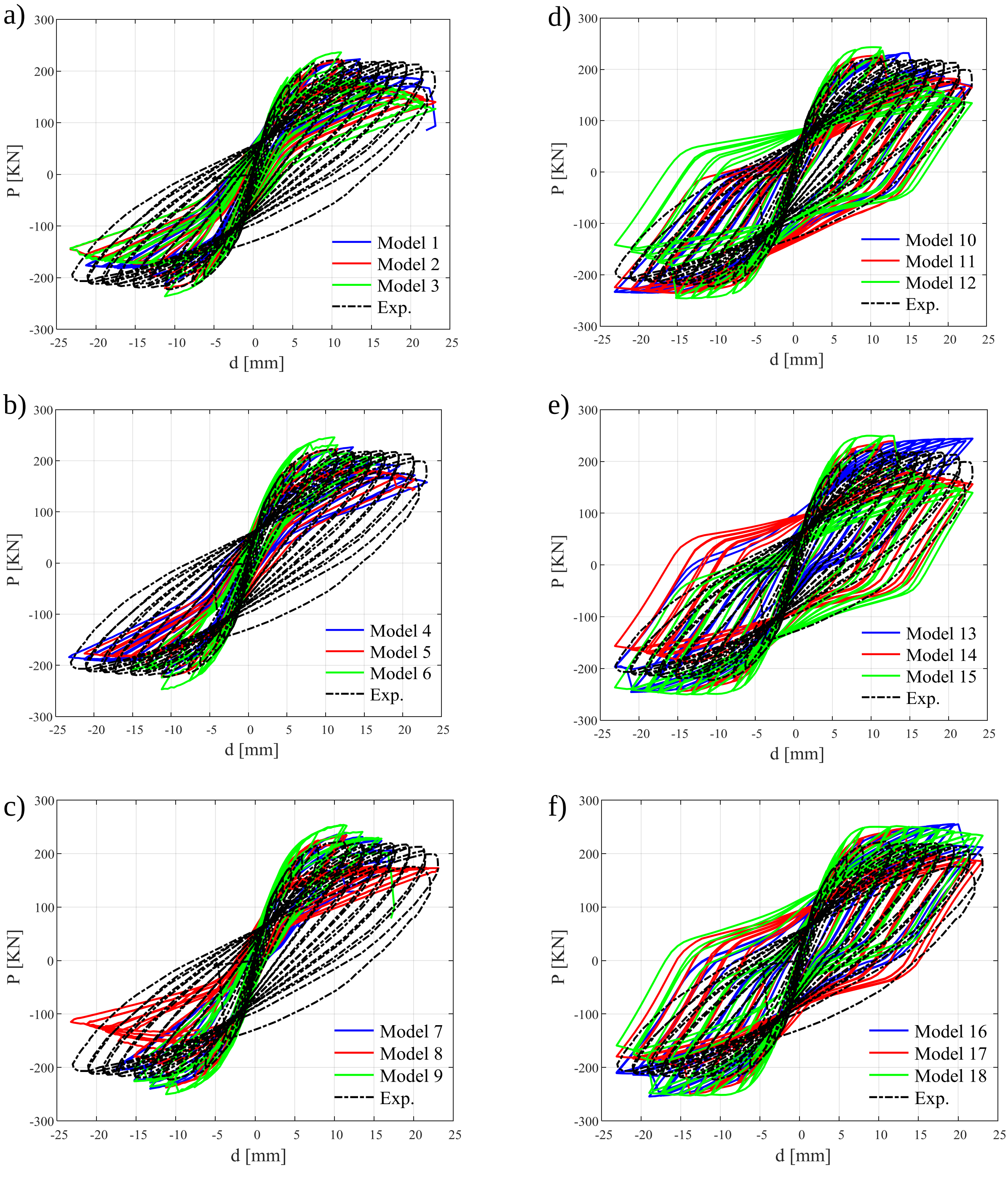

Figure 10: Load vs displacement diagrams from experimental tests SW8 of Zhang and Wang [22] and NLFEA results; (a-c) Software A, (d-f) Software B.

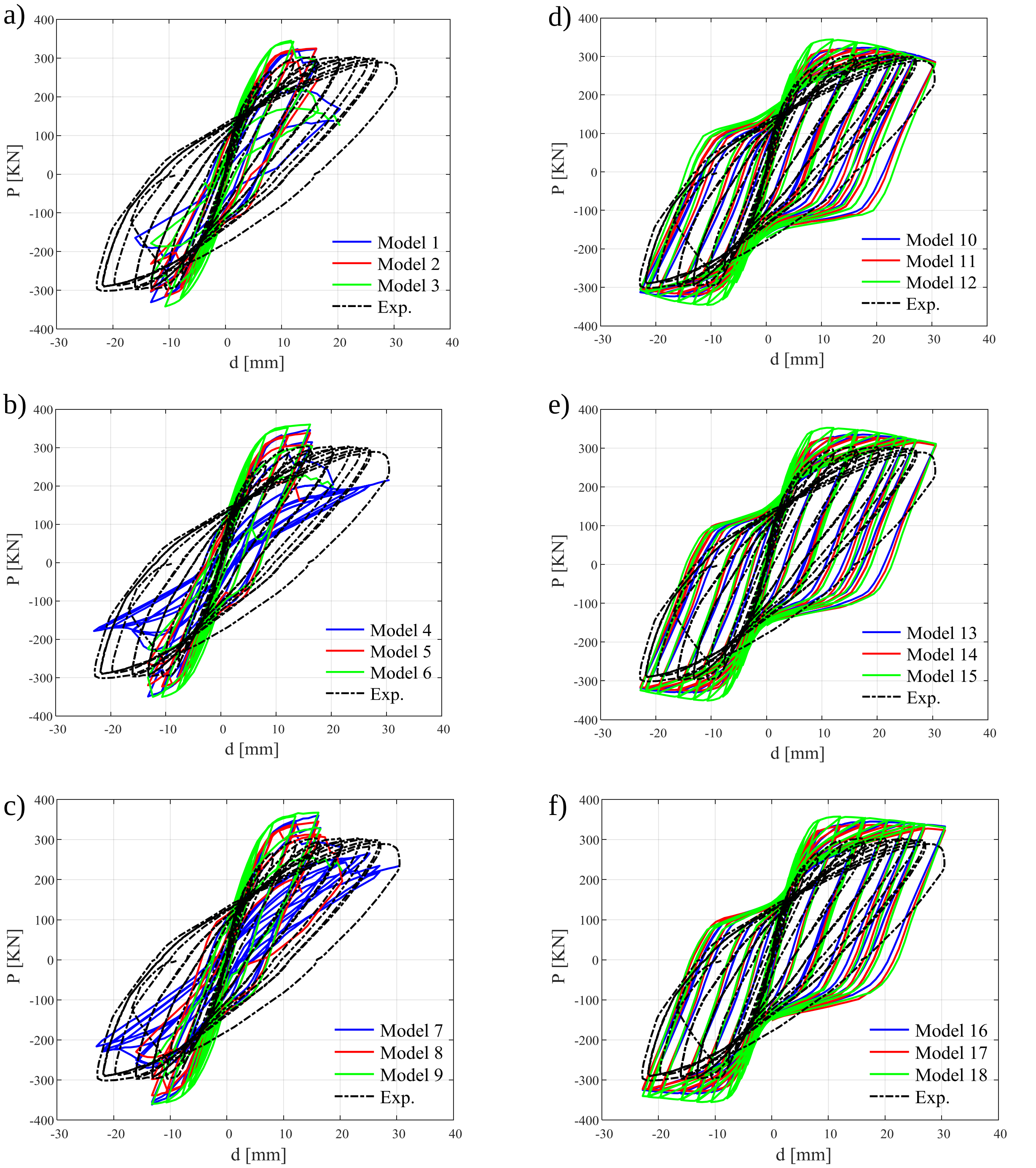

Figure 11: Load vs displacement diagrams from experimental tests SW9 of Zhang and Wang [22] and NLFEA results; (a-c) Software A, (d-f) Software B.

The results deriving from the abovementioned 162 non-linear FE simulations are useful to assess the resistance model uncertainties in 2D NLFEAs of reinforced concrete structures characterised by different failure modes under cyclic loads. These results have also demonstrated the several difficulties, which commonly occur considering different types of software and constitutive laws, in reproducing the actual failure behaviour of structural members.

5 CONCLUSIONS

This work evaluates the values of the model uncertainties (i.e., epistemic uncertainties) regarding the global structural resistance for 2D non-linear finite element method analyses of reinforced concrete systems under cyclic loads. Various experimental tests concerning different walls subject of cyclic shear action, have been numerically simulated by means of appropriate 162 NLFEAs considering two different software codes, three different constitutive laws for the behaviour of concrete in tension and three different shear behaviour after cracking. From the comparison with the experimental outcomes, the FE results have demonstrated the several difficulties, which commonly occur employing different types of software and constitutive laws, in reproducing the actual failure behaviour and the actual failure load of the all structural members considered. In general, it can be observed that a tensile behavior of the concrete perfectly plastic always gives a greater overestimation of the structural resistance, and that the variation of the shear retention factor varies the amplitude of the cycle, and therefore the dissipated energy. However, in terms of resistance, a shear retention factor close to 0.1 is the one that best fits the experimental test.

ACNOWLEDGEMENTS

This work is part of the collaborative activity developed by the authors within the framework of the Committee 3 – Task Group 3.1: *"Reliability and safety evaluation: full-probabilistic and semi-probabilistic methods for existing structures"* of the International Federation for Structural Concrete (*fib*).

REFERENCES

[1] *fib* Bulletin N°45. Practitioner's guide to finite element modelling of reinforced concrete structures – State of the art report. Lausanne; 2008.

[2] Belletti B, Damoni C, Hendriks MAN. Development of guidelines for nonlinear finite element analyses of existing reinforced and prestressed beams. European Journal of Environmental and Civil Engineering 2011;15(9): 1361-1384.

[3] DNV-RP-C208. Determination of structural capacity by non-linear FE analysis methods, Recommended Practice, DET NORSKE VERITAS AS 2013, http://www.dnv.com.

[4] Most T. Assessment of structural simulation models by estimating uncertainties due to model selection and model simplification. Computers and Structures 2011; 89(17-18): 1664-1672.

[5] Piluso V., Pisapia A., Castaldo P., Nastri E., (2019) "Probabilistic Theory of Plastic Mechanism Control for Steel Moment Resisting Frames", Structural Safety, (2019), 76:95-107, https://doi.org/10.1016/j.strusafe.2018.08.003.

[6] Basone, F., Castaldo, P., Cavaleri, L., Di Trapani, F. (2019) Response spectrum analysis of frame structures: reliability-based comparison between complete quadratic combination and damping-adjusted combination, Bulletin of Earthquake Engineering.

[7] Haukaas T, Gardoni P. Model Uncertainty in Finite-Element Analysis: Bayesian Finite Elements. Journal of Engineering Mechanics 2011; 137(8): 519-526.

[8] Allaix DL, Carbone VI, Mancini G. Global safety format for non-linear analysis of reinforced concrete structures. Structural Concrete 2013; 14(1): 29-42.

[9] Castaldo P., Gino D., Carbone V.I., Mancini G. (2018) Framework for definition of design formulations from empirical and semi-empirical resistance models, Structural Concrete, 19(4): 980-987.

[10] Castaldo P, Gino D, Bertagnoli G, Mancini G. Partial safety factor for resistance model uncertainties in 2D non-linear finite element analysis of reinforced concrete structures, Engineering Structures, 176(2018), 746-762.

[11] Shlune H, Gylltoft K, Plos M. Safety format for non-linear analysis of concrete structures. Magazine of Concrete Research 2012; 64(7): 563-574.

[12] König G, Nguyen T, Ahner C. Consistent safety format. In: CEB, editor. CEB bulletin 239 – non-linear analysis: discussion papers from the working party in commission 1. CEB 1997. Lausanne.

[13] Ftima MB, Massicotte B. Development of a reliability framework for the use of advanced nonlinear finite elements in the design of concrete structures. Journal of Structural Engineering 2012; 138:1054–64.

[14] CEN EN 1992-2 Eurocode 2 – Design of concrete structures, Part 2: concrete bridges. CEN 2005. Brussels.

[15] fib Model Code for Concrete Structures 2010. fib 2013. Lausanne.

[16] Blomfors M, Engen M, Plos M. Evaluation of safety formats for non-linear finite element analyses of statically indeterminate concrete structures subjected to different load paths. Structural Concrete 2016; 17(1): 44-51.

[17] Val D, Bljuger F, Yankelevsky D. Reliability evaluation in nonlinear analysis of reinforced concrete structures. Structural Safety 1997; 19(2): 203-217.

[18] Cervenka V. Reliability-based non-linear analysis according to fib Model Code 2010. Structural Concrete 2013; 14(1): 19-28.

[19] Kiureghian AD, Ditlevsen O. Aleatory or epistemic? Does it matter?. Structural Safety 2009; 31: 105-112.

[20] Kypros Pilakoutas and Amr Einashai. Cyclic Behaviour of Reinforced Concrete Cantilever Walls, Part I : Experimental Results. ACI structural journal no.92-S25, 1995.

[21] Ioannis D. Lefas and Micheal D. Kotsovos. Strength and deformation characteristics of reinforced concrete walls under load reversals. ACI structural journal no.87-S74, 1990.

[22] Yunfeng Zhang and Zhihao Wang. Seismic behaviour of reinforced concrete shear walls subjected to high axial loading. ACI structural journal no.97-S75, 2000.

[23] Patè-Cornell ME. Uncertainties in risk analysis: six levels of treatment, Reliability Engineering and System Safety 1996; 54: 95-111.

[24] Ditlevsen O. Model uncertainty in structural reliability. Structural Safety 1982; 1: 73-86.

[25] Bulleit WM. Uncertainty in structural engineering. Practice Periodical on Structural Design and Construction ASCE 2008; 13: 24-30.

[26] CEN. EN 1990: Eurocode – Basis of structural design. CEN 2013. Brussels.

[27] CEN. EN 1992-1-1: Eurocode 2 – Design of concrete structures. Part 1-1: general rules and rules for buildings. CEN 2014. Brussels.

[28] Allen TM , Nowak AS, Bathurst RJ. Calibration to determine load and resistance factor for geotechnical a structural design. Transport research board circular N° EC-079 2005. Washington.

[29] Holický M, Retief JV, Sikora M. Assessment of model uncertainties for structural resistance. Probabilistic Engineering Mechanics 2016; 45: 188-197.

[30] Sikora M, Holicky M, Prieto M, Tanner P. Uncertainties in resistance models for sound and corrosion-damaged RC structures according to EN 1992-1-1. Materials and structures 2014; 48: 3415-3430.

[31] Engen M, Hendriks MAN, Øverli JA, Åldtstedt E. Solution strategy for non-linear finite element analyses of large reinforced concrete structures. Str. Concrete 2015; 3: 389-397.

[32] ATENA 2D v5. Cervenka Consulting s.r.o. . Prague. Czech Republic. 2014.

[33] DIANA FEA BV. Delftechpark 19a 2628 XJ Delft. The Netherlands. 2017.

[34] Bertagnoli G, La Mazza D, Mancini G. Effect of concrete tensile strength in non –linear analysis of 2D structures: a comparison between three commercial finite element softwares. 3rd International Conference on Advances in Civil, Structural and Construction Engineering – CSCE 2015. Rome. 104-111. 10-11 December 2015.

[35] Thorenfeldt E, Tomaszewicz A and Jesen J, 1987 "Mechanical properties of high-strength concrete and applications in design", Proc. Symp. Utiliz. of High-Strength Concrete,149-159.

[36] De Borst R, Nauta P. Non-orthogonal cracks in a smeared finite element model. Engineering Computations 1985; 2: 35-46.

[37] Riggs HR, Powell GH. Rough crack model for analysis of concrete. J. Eng. Mech. Div. ASCE 1986; 112(5): 448-464.

[38] Massicotte B, Elwi AE, MacGregor JG. Tension-stiffening models for planar reinforced concrete members. Journal of Structural Engineering 199; 116(11): 3039-3058.

[39] Sykora M., Krejsa J., Mlcoch J., Prieto M., Tanner P. Uncertainty in shear resistance models of reinforced concrete beams according to *fib* MC2010, Struc. Concrete. 2018, 19(1):284-295.